PHYSICAL REVIEW B **82**, 201407(R) (2010)

Nonlinear Hall effect and multichannel conduction in $LaTiO_3/SrTiO_3$ superlattices

J. S. Kim,[1,2] S. S. A. Seo,[1,3] M. F. Chisholm,[3] R. K. Kremer,[1] H.-U. Habermeier,[1] B. Keimer,[1] and H. N. Lee[3,*]
[1]*Max-Planck-Institut für Festkörperforschung, Heisenbergstraße 1, D-70569 Stuttgart, Germany*
[2]*Department of Physics, Pohang University of Science and Technology, Pohang 790-784, Korea*
[3]*Materials Science and Technology Division, Oak Ridge National Laboratory, Oak Ridge, Tennessee 37831, USA*
(Received 20 October 2010; published 17 November 2010)

We report magnetotransport properties of heterointerfaces between the Mott insulator $LaTiO_3$ and the band insulator $SrTiO_3$ in a delta-doping geometry. At low temperatures, we have found a strong nonlinearity in the magnetic field dependence of the Hall resistivity, which can be effectively controlled by varying the temperature and the electric field. We attribute this effect to multichannel conduction of interfacial charges generated by an electronic reconstruction. In particular, the formation of a highly mobile conduction channel revealed by our data is explained by the greatly increased dielectric permeability of $SrTiO_3$ at low temperatures and its electric field dependence reflects the spatial distribution of the quasi-two-dimensional electron gas.

DOI: 10.1103/PhysRevB.82.201407 PACS number(s): 73.40.−c, 73.21.Cd, 73.50.−h

Recent advances in the design of artificial transition-metal-oxide heterointerfaces[1,2] have vastly expanded the range of materials in which electronic interface phenomena can be systematically studied and controlled. At heterointerfaces between the two band insulators $LaAlO_3$ and $SrTiO_3$, several interesting physical phenomena have been reported, including a metal-insulator transition,[3] electric field tunable switching,[3] magnetic correlations,[4] and two-dimensional (2D) superconductivity.[5,6] Since bulk transition-metal oxides show a large variety of competing ground states and diverse physical properties due to strong electron correlations, incorporating such complex oxides in heterostructures provides additional opportunities for generating novel phenomena at the interface.[7]

$LaTiO_3/SrTiO_3$ heterostructures are, in this respect, promising candidates because of several features that are distinct from those of their $LaAlO_3/SrTiO_3$ counterparts. The unpaired Ti d^1 valence electrons of $LaTiO_3$ form an antiferromagnetic Mott-insulating state due to strong electron correlations. The interfacial properties of $LaTiO_3$ are thus expected to be influenced by electronic correlations that tend to favor magnetic ground states. In fact, recent model calculations for $LaTiO_3/SrTiO_3$ interfaces proposed a magnetic and orbital order distinct from that of bulk $LaTiO_3$ in a wide range of parameter space,[7,8] which still requires experimental verification. Moreover, both $SrTiO_3$ and $LaTiO_3$ share a common constituent, the TiO_2 layer. When these two materials are stacked together at the atomic scale, this produces an electron-type $(TiO_2)^0/(LaO)^+$ interface. Importantly, Ti d^1 states in $LaTiO_3$ can readily accommodate additional holes so that direct charge transfer from this state to the $SrTiO_3$ d^0 state can occur at the interface.[1] Even a single $LaTiO_3/SrTiO_3$ interface can therefore be conducting.

In order to realize electronically reconstructed $LaTiO_3/SrTiO_3$ heterostructures, we fabricated various superlattices composed of unit-cell-thin $LaTiO_3$ layers epitaxially embedded in a $SrTiO_3$ matrix [Fig. 1(a)] on atomically flat (001) $SrTiO_3$ substrates, analogous to the delta-doping geometry in conventional semiconductor heterostructures.[9] Well-defined oscillations of the reflection high-energy electron-diffraction (RHEED) pattern [Fig. 1(b)] and pronounced superlattice peaks from x-ray diffraction scans[9] as well as the sharp interfaces in Z-contrast scanning transmission electron microscopy images [Figs. 1(c) and 1(d)] clearly confirm that the unit-cell-thin $LaTiO_3$ layers are sharply confined within the $SrTiO_3$ matrix.

The temperature dependence of the two-dimensional resistance (R_{2D}) for various superlattices demonstrates the presence of conducting interfaces [Fig. 2(a)], consistent with recent results from photoemission[10] and optical spectroscopy.[11] As to the origin of such metallic interfaces, one can consider two possible scenarios; (1) interfacial charge-carrier doping driven by an electronic reconstruction and (2) growth-induced extrinsic chemical doping, e.g., off-stoichiometry of oxygen. While still controversial, the growing consensus is that extrinsic doping by oxygen vacancies can be avoided by fabricating superlattices in an oxygen-rich environment and/or postannealing at a high oxygen pressure.[12–17] Such systems have revealed a 2D carrier density (n_{2D}) of about 10^{14} cm^{-2}, and weak temperature dependence of $R_{2D}(T)$.[4,12,16] As one can see in Figs. 2(a) and 2(b), our $LaTiO_3/SrTiO_3$ superlattices indeed show these features. Furthermore, neither R_{2D} nor n_{2D} for our superlattices exhibit

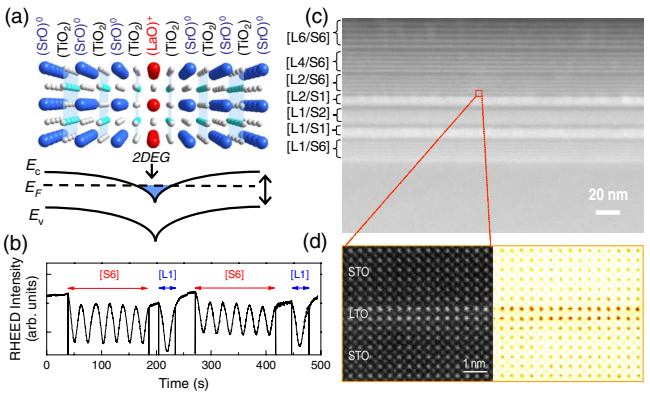

FIG. 1. (Color online) (a) Schematic representation of a delta-doped $LaTiO_3/SrTiO_3$ heterostructure and its energy band diagram. The superlattices are denoted as [Lm/Sn], where L(S) refers to $LaTiO_3$ ($SrTiO_3$), and $m(n)$ indicates its thickness in unit cells. (b) RHEED oscillations during the growth of a [L1/S6] superlattice. (c) Cross-sectional Z-contrast image of a test sample with various [Lm/Sn] superlattices. (d) High-resolution Z-contrast image of a [L2/S6] superlattice (left) and its colorized version (right).

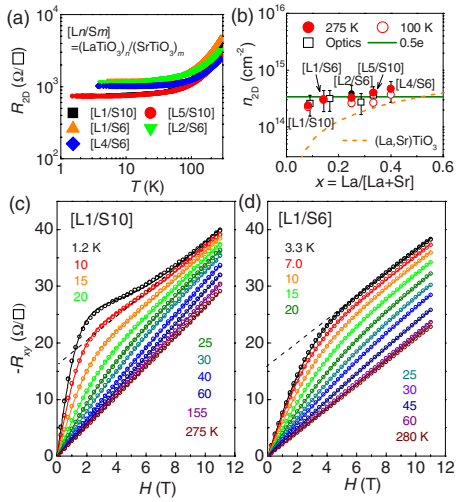

FIG. 2. (Color online) (a) Temperature dependence of 2D resistance per interface $R_{2D}=R_{sheet}N_{IF}$ for various configurations, where R_{sheet} and N_{IF} are the sheet resistance and the number of interfaces, respectively. (b) The carrier density per interface, $n_{2D}=n_{sheet}/N_{IF}$, at $T=100$ and 275 K as a function of La fraction where the sheet carrier density $n_{sheet}=-1/R_H e$. For comparison, we also plotted the carrier density obtained from optical spectroscopy (Ref. 11), the induced charge, $0.5e$ per unit cell (solid line), which is nominally expected to be transferred across the interfaces and the charge density (dashed line) for $(La,Sr)TiO_3$ solid solutions (Refs. 18 and 19). [(c) and (d)] $R_{xy}(H)$ at various temperatures for [L1/S10] and [L1/S6] superlattices. The solid lines are fitted curves using the two-channel model. The dashed lines indicate the result of a linear fit of the high-field $R_{xy}(H)$ data.

any dependence on the global cation stoichiometry, i.e., the La fraction, $x=\mathrm{La}/(\mathrm{La}+\mathrm{Sr})$. In particular, n_{2D} exhibits only a narrow range of values, unlike $(La,Sr)TiO_3$ alloys where it depends strongly on x.[18,19] Based on this evidence, we therefore rule out a major influence of oxygen vacancies and/or chemical mixing on the electronic properties of our superlattices.

To reveal the nature of the interfacial charge conduction, we have investigated the low-temperature transport properties, in particular, the magnetic field (H) dependence of the Hall resistance $R_{xy}(H)$. Figures 2(c) and 2(d) show $R_{xy}(H)$ at different temperatures for [L1/S10] and [L1/S6] superlattices. $R_{xy}(H)$ is negative and depends linearly on H above 50 K, as found in conventional metals. At lower temperatures, however, $R_{xy}(H)$ exhibits a pronounced nonlinearity: $-R_{xy}(H)$ rises rapidly with increasing H, shows a broad hump in some cases, and finally crosses over to linear H dependence at high magnetic fields. A similar behavior has also been observed in other superlattices.[9] Since such a strong nonlinearity in $R_{xy}(H)$ has not been observed in bulk $LaTiO_3$ nor in $SrTiO_3$, these observations suggest a novel interfacial state in $LaTiO_3/SrTiO_3$ heterostructures.

At first glance, it is tempting to consider the anomalous Hall effect (AHE), often found in ferromagnetic metals,[20] as the origin of this behavior. In fact, the AHE has recently been invoked to explain transport anomalies in related systems such as Cr-doped bulk $(La,Sr)TiO_3$ (Ref. 21) and $LaVO_3/SrTiO_3$ heterostructures.[22] Several of our observations are, however, inconsistent with this interpretation. First, we have not observed any magnetic hysteresis, which would be expected if ferromagnetism were present.[9] Second, if the effects were due to spin textures at the interface of $LaTiO_3$, as suggested for $LaVO_3/SrTiO_3$ superlattices,[22] it would be natural to expect that the characteristic temperature T_0, where the nonlinearity of $R_{xy}(H)$ becomes significant, is strongly dependent on the carrier density. In bulk $LaTiO_3$, for instance, the Néel temperature $T_N \sim 140$ K is dramatically reduced to zero at a doping level of a few percent.[18,19] However, T_0 of our superlattices is almost independent on n_{2D} over a rather wide range.[9] These findings have prompted us to consider an alternative origin of the nonlinear $R_{xy}(H)$, even though we cannot rule out the possibility of interfacial magnetism due to orbital or charge ordering.[7,8]

A nonlinear Hall effect can also arise from a multichannel conduction involving different electronic bands and/or spatially separated parallel conducting channels.[20] Although it is usually much weaker than what we observed in our $LaTiO_3/SrTiO_3$ heterostructures, a nonlinear Hall effect has been found in delta-doped semiconductors.[23] For high-doping concentration, multiple subbands inside the potential well due to the delta doping are occupied and are involved in the charge conduction. The mobility for each subband is quite sensitive to the spatial distribution of carriers; the wave function of the lower (higher) subbands experiences higher (lower) scattering because of larger (smaller) overlap with the dopant layer. We note that we do not exclude a possibility of potential contribution of the scattering dominated by dislocations or defects in the atomically thin $(LaO)^+$ layer, arising, e.g., from the presence of the out-of-plane lattice mismatch near the step-and-terrace structure. Nevertheless, when only two contributions to conduction are taken into account, the $R_{xy}(H)$ can be written as $R_{xy}(H) = [(\mu_1^2 n_1 + \mu_2^2 n_2) + (\mu_1\mu_2 B)^2(n_1 + n_2)]/\ e[(\mu_1|n_1| + \mu_2|n_2|)^2 + (\mu_1\mu_2 B)^2(n_1+n_2)^2]$. Based on this equation, we have fitted the $R_{xy}(H)$ data with the constraint of $R_{xx}(0)=1/e(n_1\mu_1 + n_2\mu_2)$. The strong nonlinearity of $R_{xy}(H)$, including, the characteristic features at low magnetic fields, are well captured by the fit of $R_{xy}(H)$ (see Fig. 2), suggesting that a similar mechanism is at work in oxide heterostructures.[24]

What is unique in the $LaTiO_3/SrTiO_3$ system, compared to conventional semiconductor heterostructures, is the strong temperature dependence. Figure 3 shows the results of the temperature-dependent fitting parameters. The fit implies a large difference in both the density and the mobility of majority (n_1, μ_1) and minority (n_2, μ_2) carriers. For all samples, the density n_1 of the majority carriers is almost independent on temperature while their mobility μ_1 increases upon lowering the temperature. On the other hand, the minority carrier density n_2 exhibits strong temperature dependence and it appears too small ($<10^{10}$ cm^{-2}) to be detected by our Hall measurements at high temperatures. Below 50 K, however, it starts to grow rapidly by an order of magnitude before saturating at low temperatures. The temperature dependence of μ_2 is similar to that of μ_1, but its magnitude is 10^2 times greater, reaching 1000–5000 cm^2 V^{-1} s^{-1} at low temperatures.

Moreover, such a strong enhancement of the mobility of the minority carriers cannot be simply explained by usual

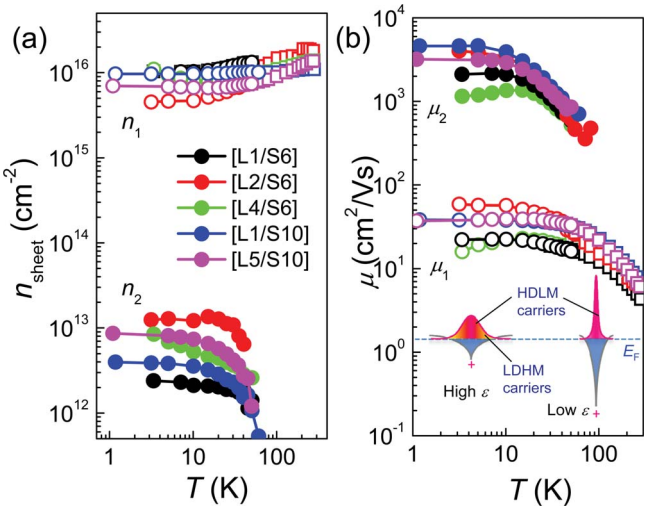

FIG. 3. (Color online) The temperature dependence of sheet carrier densities n_i and mobilities μ_i $(i=1,2)$ assuming a two-channel conduction in various $LaTiO_3/SrTiO_3$ superlattices. The majority charge carriers (open circles) have lower mobility while the minority charge carriers (solid circles) have much higher mobility. At high temperatures, where $R_{xy}(H)$ shows almost linear field dependence (Fig. 2), we estimate the density and the mobility (open squares) for one type of charge carriers, which corresponds to the majority charge carriers. Schematics of the potential profile and wave function of charge carriers are shown in the inset. The LDHM and HDLM carriers stand for the low-density-high-mobility and high-density-low-mobility carriers, respectively. The higher dielectric constant ε of $SrTiO_3$ at low temperatures (left) makes the potential profile much shallower than that at high temperatures (right).

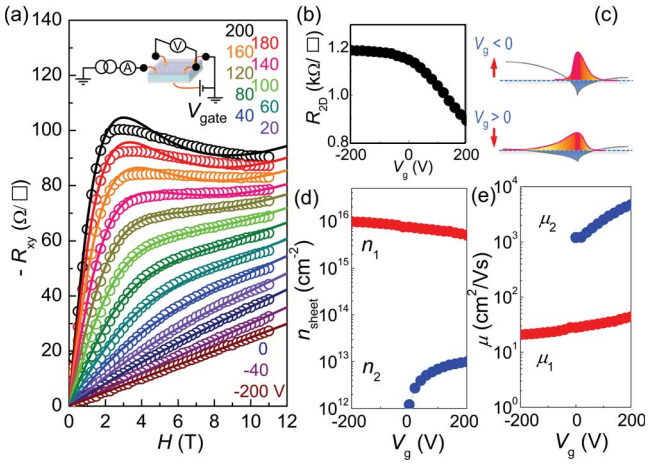

FIG. 4. (Color online) (a) Hall resistance of a [L2/S6] superlattice as a function of magnetic field at $T=3$ K for various gate voltages increasing with a 20 V step between −200 and 200 V. The gate electric field was applied across the 0.5-mm-thick $SrTiO_3$ substrate through backside contacts. The solid lines are fitted curves using the two-channel model. (b) Gate voltage dependence of the 2D resistance. (c) Schematics of the effects of external electric field on the potential profile and wave function of charge carriers in a delta-doped superlattice. Here the gate electrode is assumed to be placed on the left side of the delta-doped layer. [(d) and (e)] The gate voltage dependence of carrier densities and mobilities for the two-channel conduction.

thermal effects, e.g., reduced electron-phonon scattering at low temperatures. The increasing minority carrier density, n_2, at low temperatures is also quite unusual. In the aforementioned model, the minority carrier density depends on how far the wave function is extended on either side of the potential well. A rough estimate[23] of the spatial extent, z, for the ground-state wave function in a V-shape quantum well is $z \sim (\hbar^2 \varepsilon / e^2 N_D^{2D} m^*)^{1/3}$. Here, N_D^{2D} is the density of dopants and m^* is the effective mass of the carriers, which are usually temperature independent. On the other hand, the characteristic width of the carrier distribution also depends on the strength of potential screening, i.e., the dielectric permittivity ε. In contrast to conventional semiconductors, ε of $SrTiO_3$ increases by two orders of magnitude at low temperatures due to incipient ferroelectricity.[25] With the enhanced ε at low temperatures, the screening of the electric field introduced by delta doping becomes more effective, and the wedge-shaped potential becomes shallower, as illustrated in the inset of Fig. 3. Accordingly, the weight of charge distribution away from the delta-doping layer increases, effectively leading to an increase in the minority carrier density. The increase in the minority carrier density is indeed quite similar to the temperature dependence in ε for bulk $SrTiO_3$.[25]

Further evidence for the close relationship between the carrier mobility and its spatial distribution is confirmed by investigating the effect of a gate voltage (V_g). Figures 4(a) and 4(b) show that the variation in V_g induces a large modulation of both $R_{xy}(H)$ and R_{2D} measured from a [L2/S6] superlattice. For a large negative V_g, corresponding to the more resistive state, $R_{xy}(H)$ shows approximately linear dependence on the magnetic field. As V_g increases toward positive biasing, R_{2D} is gradually reduced [Fig. 4(b)] and the nonlinearity of $R_{xy}(H)$ becomes remarkably stronger. The crossover from linear to nonlinear behavior of $R_{xy}(H)$ with increasing V_g resembles the temperature dependence of $R_{xy}(H)$ (Fig. 2), suggesting that the two-channel model can be applied here as well. Indeed, fits of the two-channel model to the data at different V_g again yield good agreement [Fig. 4(a)]. The gate voltage dependence of the transport parameters extracted from these fits is presented in Figs. 4(d) and 4(e). While the density n_1 and mobility μ_1 of the majority carriers do not depend very much on V_g, the corresponding quantities of the minority carriers exhibit much stronger dependence on V_g. In particular, n_2 increases by an order of magnitude at high positive V_g and μ_2 is significantly enhanced up to 5000 cm^2 V^{-1} s^{-1}. For negative V_g, on the other hand, n_2 quickly becomes negligible.

In the framework of the model discussed above, the origin of this behavior is readily explained as the confluence of two factors: first, ε of $SrTiO_3$ is known to decrease in an external electric field.[25] The applied electric field reverses the increase in ε at low temperatures noted above, thus reducing n_2 for negative V_g. For positive V_g, this effect is offset by a second factor, namely the flattening of the potential profile toward the gate electrode, as illustrated in Fig. 4(c). The shallower potential profile shifts the electron wave function away from the scattering centers in the delta-doping layer, thereby enhancing the density and mobility of the minority carriers. Moreover, considering our superlattice geometry with a maximum 2–3 nm (6 unit cells) separation between

two adjacent $LaTiO_3$ layers, we expect that most of the minority carriers with a high mobility reside near the first interface from the $SrTiO_3$ substrate because the electric field applied through the back gate affects dominantly the first interface with the substrate (see Ref. 9 for more details). These results clearly demonstrate that the observed two-channel transport in our $LaTiO_3/SrTiO_3$ heterostructures reflects the spatial extent of the quasi-2D electron gas, which can be modulated by the external electric field.

Previously, the spread of charge carriers at room temperature has been reported to be approximately three unit cells ($\sim$1 nm).[1] Based on our results, it is expected to be wider at low temperatures due to the drastic increase in ε for $SrTiO_3$. For $LaAlO_3/SrTiO_3$ heterostructures, a penetration depth of carriers, i.e., 10 nm at 10 K, has been estimated.[26] However, we note that unlike $LaAlO_3$, the $LaTiO_3$ layer is a d^1 charge reservoir and can accommodate extra charges. The exact spatial distribution of the carriers and their redistribution under electric fields need to be further investigated, especially for the highly mobile conduction channel.

In summary, we have shown how the transport properties of the 2D electron gas at an interface of $LaTiO_3/SrTiO_3$ can be modulated by delta doping and an external electric field. Although the effect of electronic correlations in our superlattices is suppressed by a leakage of the Ti d^1 electrons of $LaTiO_3$ into $SrTiO_3$, diminishing the tendency toward magnetism, our finding provides new perspectives for wave-function engineering in oxide heterostructures. We also envision that bulklike antiferromagnetism can be recovered by increasing the thickness of the $LaTiO_3$ layers, which may add another degree of freedom to manipulate the intriguing electronic properties of the electronically reconstructed interface. Thus, further studies on the response of other degree of freedoms, e.g., spin or orbital for $LaTiO_3/SrTiO_3$ interfaces are desirable to clarify the detailed nature of the interface and possible relevance of the interfacial magnetism.

We thank K. B. Lee and S. Okamoto for useful discussions and comments. The work at ORNL was supported by the Division of Materials Sciences and Engineering, U.S. Department of Energy. The work at POSTECH was supported by the National Research Foundation of Korea through Basic Science Research Program (Grant No. 2009-0076700). We also acknowledge support by the DFG under Grant No. SFB/TRR 80.

*hnlee@ornl.gov

[1] A. Ohtomo, D. A. Muller, J. L. Grazul, and H. Y. Hwang, Nature (London) **419**, 378 (2002).
[2] H. N. Lee, H. M. Christen, M. F. Chisholm, C. M. Rouleau, and D. H. Lowndes, Nature (London) **433**, 395 (2005).
[3] S. Thiel, G. Hammerl, A. Schmehl, C. W. Schneider, and J. Mannhart, Science **313**, 1942 (2006).
[4] A. Brinkman, M. Huijben, M. Van Zalk, J. Huijben, U. Zeitler, J. C. Maan, W. G. Van Der Wiel, G. Rijnders, D. H. A. Blank, and H. Hilgenkamp, Nature Mater. **6**, 493 (2007).
[5] N. Reyren, S. Thiel, A. D. Caviglia, L. Fitting Kourkoutis, G. Hammerl, C. Richter, C. W. Schneider, T. Kopp, A.-S. Rüetschi, D. Jaccard, M. Gabay, D. A. Muller, J.-M. Triscone, and J. Mannhart, Science **317**, 1196 (2007).
[6] A. D. Caviglia, S. Gariglio, N. Reyren, D. Jaccard, T. Schneider, M. Gabay, S. Thiel, G. Hammerl, J. Mannhart, and J.-M. Triscone, Nature (London) **456**, 624 (2008).
[7] S. Okamoto and A. J. Millis, Nature (London) **428**, 630 (2004).
[8] S. S. Kancharla and E. Dagotto, Phys. Rev. B **74**, 195427 (2006); R. Pentcheva and W. E. Pickett, Phys. Rev. Lett. **99**, 016802 (2007).
[9] See supplementary material at http://link.aps.org/supplemental/10.1103/PhysRevB.82.201407 for the details of growth conditions, characterizations, and results on other samples.
[10] M. Takizawa, H. Wadati, K. Tanaka, M. Hashimoto, T. Yoshida, A. Fujimori, A. Chikamatsu, H. Kumigashira, M. Oshima, K. Shibuya, T. Mihara, T. Ohnishi, M. Lippmaa, M. Kawasaki, H. Koinuma, S. Okamoto, and A. J. Millis, Phys. Rev. Lett. **97**, 057601 (2006).
[11] S. S. A. Seo, W. S. Choi, H. N. Lee, L. Yu, K. W. Kim, C. Bernhard, and T. W. Noh, Phys. Rev. Lett. **99**, 266801 (2007).
[12] G. Herranz, M. Basletic, M. Bibes, C. Carretero, E. Tafra, E. Jacquet, K. Bouzehouane, C. Deranlot, A. Hamzic, J.-M. Broto, A. Barthelemy, and A. Fert, Phys. Rev. Lett. **98**, 216803 (2007).
[13] W. Siemons, G. Koster, H. Yamamoto, W. A. Harrison, G. Lucovsky, T. H. Geballe, D. H. A. Blank, and M. R. Beasley, Phys. Rev. Lett. **98**, 196802 (2007).
[14] A. Kalabukhov, R. Gunnarsson, J. Börjesson, E. Olsson, T. Claeson, and D. Winkler, Phys. Rev. B **75**, 121404(R) (2007).
[15] M. Basletic, J.-L. Maurice, C. Carrétéro, G. Herranz, O. Copie, M. Bibes, É. Jacquet, K. Bouzehouane, S. Fusil, and A. Barthélémy, Nature Mater. **7**, 621 (2008).
[16] H. Y. Hwang, A. Ohtomo, N. Nakagawa, D. A. Muller, and J. L. Grazul, Physica E **22**, 712 (2004).
[17] S. S. A. Seo, Z. Marton, W. S. Choi, G. W. J. Hassink, D. H. A. Blank, H. Y. Hwang, T. W. Noh, T. Egami, and H. N. Lee, Appl. Phys. Lett. **95**, 082107 (2009).
[18] Y. Tokura, Y. Taguchi, Y. Okada, Y. Fujishima, T. Arima, K. Kumagai, and Y. Iye, Phys. Rev. Lett. **70**, 2126 (1993).
[19] Y. Taguchi, T. Okuda, M. Ohashi, C. Murayama, N. Môri, Y. Iye, and Y. Tokura, Phys. Rev. B **59**, 7917 (1999).
[20] C. Hurd, *The Hall Effect in Metals and Alloys* (Plenum Press, New York, 1972).
[21] D. Satoh, K. Okamoto, and T. Katsufuji, Phys. Rev. B **77**, 121201(R) (2008).
[22] Y. Hotta, T. Susaki, and H. Y. Hwang, Phys. Rev. Lett. **99**, 236805 (2007).
[23] E. F. Schubert, *Delta-Doping of Semiconductors* (Cambridge University Press, Cambridge, 1996).
[24] Z. S. Popovic and S. Satpathy, Phys. Rev. Lett. **94**, 176805 (2005).
[25] M. A. Saifi and L. E. Cross, Phys. Rev. B **2**, 677 (1970); T. Sakudo and H. Unoki, Phys. Rev. Lett. **26**, 851 (1971).
[26] A. Dubroka, M. Rössle, K. W. Kim, V. K. Malik, L. Schultz, S. Thiel, C. W. Schneider, J. Mannhart, G. Herranz, O. Copie, M. Bibes, A. Barthélémy, and C. Bernhard, Phys. Rev. Lett. **104**, 156807 (2010).